

Optical methods in wind tunnel flow visualization

Slavica Ristić

Leading research engineer
MTI, Belgrade, SCG

This paper reports the application of optical methods: shadow, schlieren and holographic interferometry in wind tunnel flow visualization. Some examples obtained in the MTI wind tunnels are presented. The comparative advantages of holographic method in regard to shadow and schlieren method for quantitative flow field test are analyzed.

Keywords: flow visualization, optical methods, wind tunnel

1. INTRODUCTION

Rapid advances made during the past decades on problems associated with high speed flight have brought into focus the need for competent treatment of the fundamental aspects of the aerodynamics and the need for application of basic sciences in solving actual problems. The different physical methods and techniques are employed to measure density, pressure, velocity and temperature in gas dynamics.

Flow visualization is an important tool in experimental fluid mechanics, which can provide the overall picture of an entire flow field [1-6]. Air flow around aerodynamical models is a very complex phenomenon. In optical sense, fluid flow field is a transparent object with complex distribution of light refraction index. Light beam, passing through such an environment, suffers changes in its direction and phase, so that the information in it is carried as displacements or phase modulations. Light refraction index n is the function of air density ρ in each point, $\rho(x, y, z)$. The density, on the other side, is the function of velocity V , pressure P and air temperature T [2,4].

The three principal optical methods for flow visualization are: shadow, schlieren and interferometry. There are systematic differences between these methods, since shadowgraph is sensitive to changes of the second derivative of density, schlieren to changes of density first derivative, and the interferometry is capable to measure absolute density changes [1].

The examples of the flow visualization, obtained in MTI wind tunnels, with three mentioned methods are analyzed and their advantages are pointed out.

2. TEST DESCRIPTION

In order to demonstrate and compare advantages of optical methods in complex flow field visualization, a series of experiments were performed in trisonic wind tunnel T-36, with $M_\infty = 0.7$ to 3.24. Wind tunnel test section has windows with diameter of 300 mm (pair

windows are made of glass BK7, schlieren quality and another pair of klirit) which allows the usage of optical methods, for 2D and 3D models.

Holographic interferometer with parallel beams is at the same time a schlieren and a shadow device. The schematic diagram of the experimental setup is shown in Fig. 1 [4]. The ruby laser (Apollo model 22, $E = 3 \text{ J}$, $t = 3 \text{ ns}$, $l_c = 1 \text{ m}$) (2) is used as a recording light source, while 6 mW He-Ne laser (3) is used for interferometer setting and reconstruction of holograms (9). The Hg lamp (13), small mirror (14), horizontal knife edge (15) and still camera (16) are the different parts belonging to schlieren device with Z-shape. The large concave mirrors ($D = 300 \text{ mm}$, $F = 2750 \text{ mm}$) (6) are for both systems. The shadow effects are recorded without second large mirror (6). Instead of it, a still or video camera are placed. Laser and Hg lamp are both used as light sources for shadow technique. Some mirrors, beam splitters and lenses are used for laser beams directed, enlarged, colimated and focusing (4,5,7). The lasers and all other mechanical and optical components are fixed on the adjusting platform (1) with height equal to height of wind tunnel axis (11).

Double exposition technique is used for holographic interferograms. Hologplate is exposed two times: wind off (when there exists homogeneous flow field distribution) and wind on (when there is a complex flow field for testing [1-14]. Stagnation pressure (P_0), atmospheric pressure (Pa), and Mach number (M_∞) are measured by the basic, primary measurement system (PMS) in wind tunnel at the moment of hologram or schlieren recording [4-8].

3. RESULTS AND DISCUSSION

The shadowgraph is not a method suitable for quantitative density measurements, since such evaluation would require of one to perform a double integration of the light intensity distribution over the field picture [1,5,6]. This is a convenient method to get a quick survey of the shock waves geometry, boundary layers, expansion fans and turbulence. The shadowgraph in this article (Figure 2, 3a and 4a) gives only qualitative visualization.

The quantitative evaluation of the schlieren image is based on densitometry. The distribution of the deflection angles in the test field can be calculated from densitogram in the parts of the schlieren image which is

Received: September 2005, Accepted: November 2005.

Correspondence to: Slavica Ristić

VTI,

Ratka Risanovića 1, 11000 Belgrade 35, Serbia

E-mail: slavce@yahoo.com

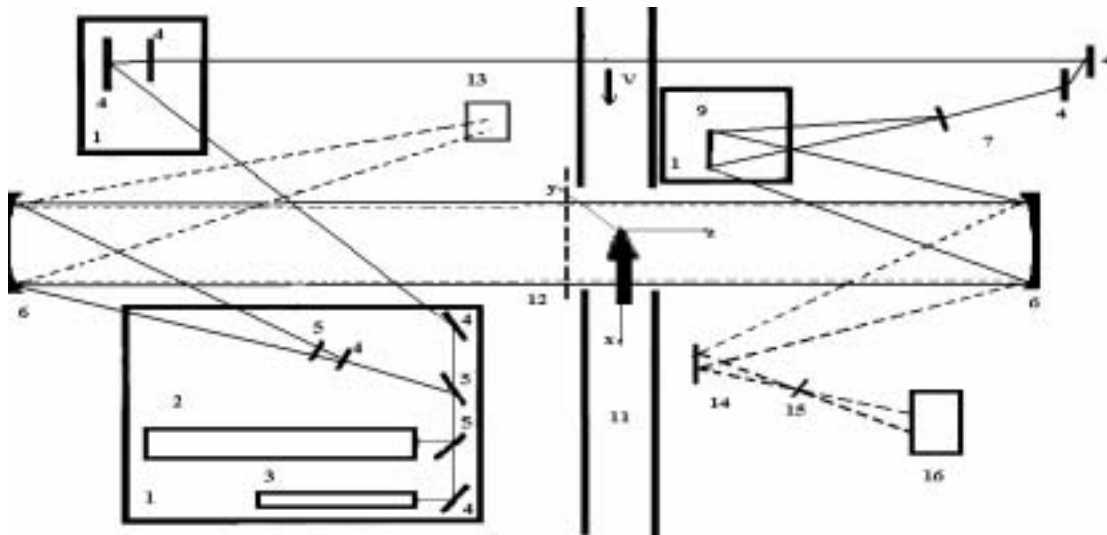


Figure 1. Schematic diagram of the device for optical methods application: holographic interferometer, schlieren and shadow device

not disturbed by light diffraction. But, the schlieren method produces a two dimensional image of a three dimensional flow field, and the computation of the density distribution $\rho(x,y,z)$ from the recorded intensity pattern is a more or less insoluble problem [1,3,5]. For schlieren test the optical parts (mirrors, lenses, windows) of the system should be as nearly perfect as possible. The interpretation of schlieren effects is closely related to knowledge of geometrical system characteristic. For those reasons, today, schlieren tests are used often for qualitative flow visualization in wind tunnels, in the same sense as the shadow method, but with a much higher degree of resolution and sensitivity [1,5,6]. Contemporary schlieren devices have a lot of modifications and improvements described in the literature [1,5].

Table 1. Flow parameters during holograms recording for model wedge and step

model	M_∞	P_0 (mbar)	P_s (mbar)	P_{at} (mbar)	T (K)
wedge	0.627	967.61	742.33	998.5	297.61
step	0.596	971.12	764.2	1000.4	293.87

3.1 Testing of 2D models

The pair of klirit windows for wind tunnel T-36 is specially made with the side model holders. 2D models (wedge, cylinder and step) are fixed in windows. Table 1. contains the flow parameters during the shadow and holographic recordings. Fig 2 is the combination of shadowgraf (lower part) and holographic interferogram (upper part) of the flow around wedge model with $M_\infty=0.627$. The stagnation point, boundary layer and the expansion waves on the rear end edges are visible. Figure 3a is the shadowgraf and 3b holographic interferogram of the flow around the step. There are visible shock waves, separation of boundary layers,

compression waves, expansion regions limited by Mach waves, the mixed layers and the recirculated flow [4-6].

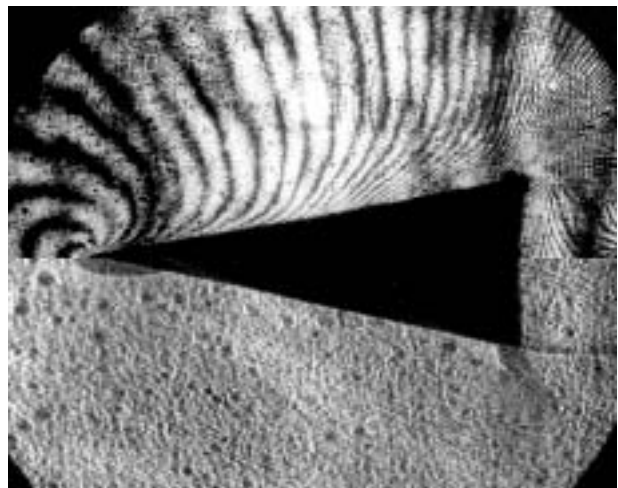
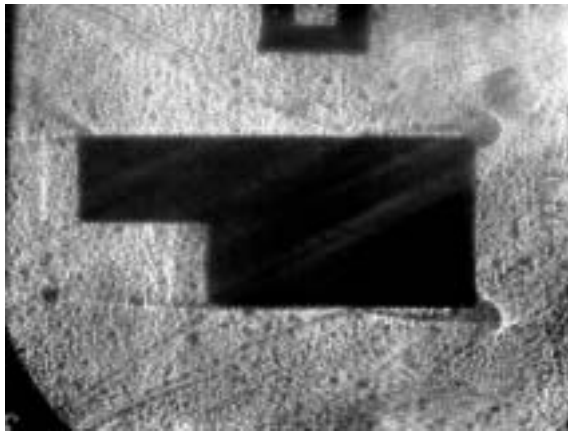


Figure. 2 Axisymmetric flow around 2D wedge, $M_\infty = 0.627$ (upper part is the interferogram, above is shadow picture)

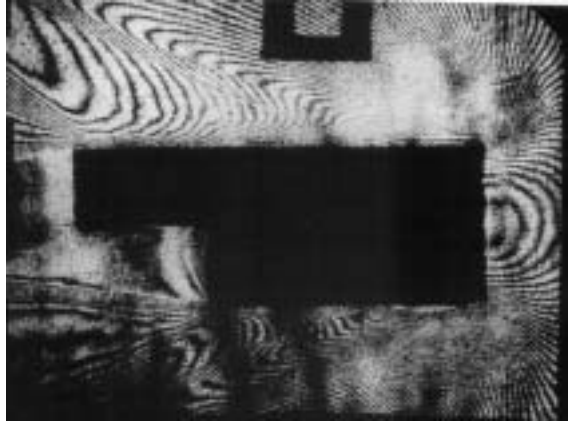
3.2 2D nozzle of missile

The complex flow in two dimensional model of rocket nozzle is tested by three optical methods. Pressure taps mounted on the upper and lower nozzle wall, and electrical scanivalves measure the pressure distribution [4,9].

The configuration of the nozzle can be changed and completed with barriers (spoiler, deflector and cone shaped barrier) serving for the control of the thrust vector. The simplest flow in the nozzle is when there are not the barriers. The flow visualization results are presented in figure 4: holographic interferogram and shadow (a), holographic interferogram and shlieren (b), holographic interferogram and theoretical isomach line in supersonic nozzle (c). It is evident that most information about flow in the nozzle is given by the interferogram.



a)



b)

Figure 3. Shadow (a) and holographic interferogram (b) of the flow around 2D step for $M_\infty = 0.596$

The interferometric fringes distribution in the nozzle image without barrier is symmetrical with respect to the nozzle axis. Fringes connect the point with equal air density (fig. 4). Interferogram is used for quantitative flow analysis. The numerical results (table 2) are compared to the results of the distribution pressure measurements on the upper and bottom wall of the nozzle (between points A and B, fig. 4c).

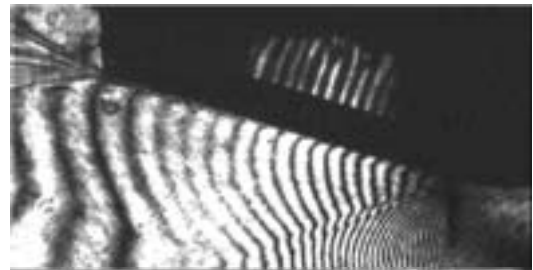
Complex flow field in the nozzle is simulated on a computer by applying the method of characteristics. (Fig 4c). The identity of the experimental and theoretical isomach lines is evident. The theoretical value of Mach number in the output plane of the nozzle is estimated to be $M=2.6$. Using the pressure measurement data, it is obtained $M=2.46$. Holographic calculations confirm that Mach number is $M=2.56$. Method of characteristics in the point B (fig 4c) gives $M=2.55$.

The placing of barriers in the supersonic flow, leads to the appearance of the stagnation zone, shock and expansion waves. The flow becomes unsymmetrical; shock wave and separation zone on the bottom wall appear. All these effects can be qualitatively and quantitatively investigated by holographic interferometry [4,9].

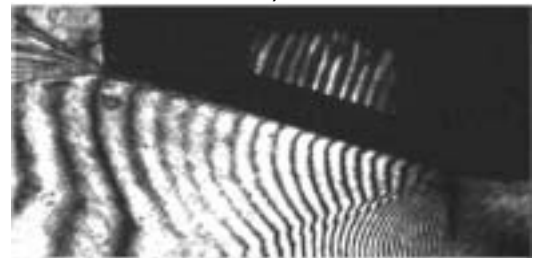
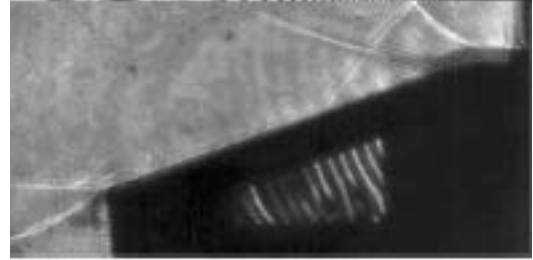
3.3 Expansion flow

The holographic interferograms were used for numerical calculation of flow field parameters in the

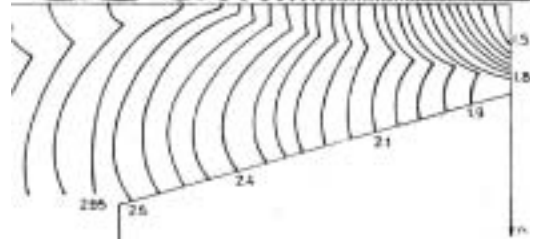
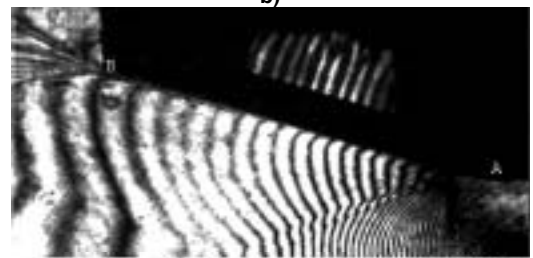
vicinity of nozzle edge, where the expansion fan is formed (E, fig. 5a) [8]. The fringe number N was read from the hologram. Points in front of expansion fan



a)



b)



c)

Figure 4. Comparative representation of supersonic flow in two dimensional model of the rocket nozzle: holographic interferogram and shadow (a), holographic interferogram and shlieren (b), holographic interferogram and theoretical isomach line in supersonic nozzle (c)

(area E, point 1, $M_\infty = 1.56$) have $N = 0$, since the last fringe (area B, point 2) has $N = 17$. The theoretical and experimental values of Mach number in the expansion area are in good agreement $M_{\text{exp}} = 2.15$, $M_{\text{the}} = 2.13$. The some region of flow is visualised with schlieren method (fig 5b) [5].

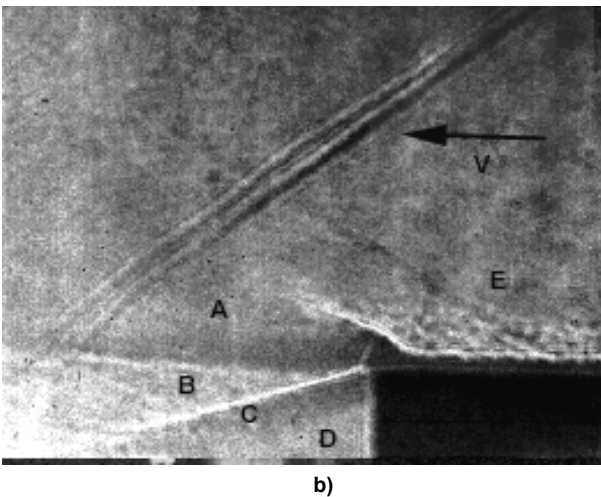
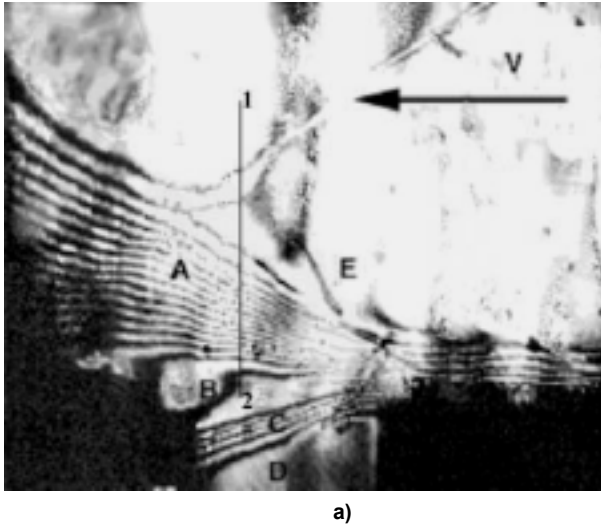
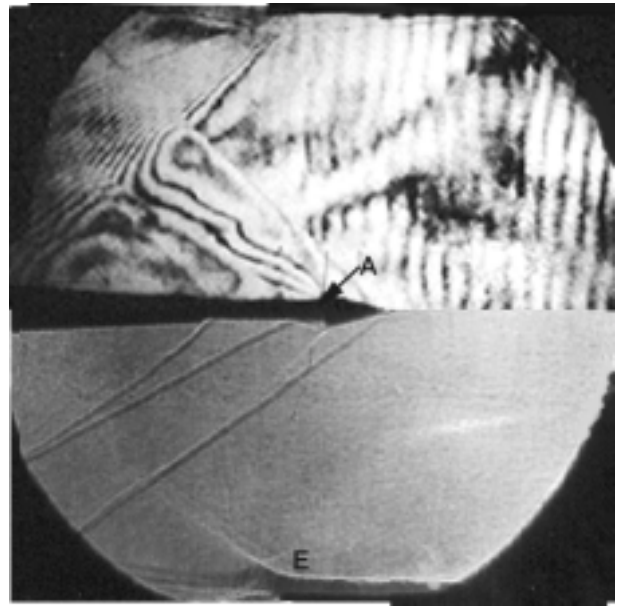


Figure 5. Interferometric (a) and schlieren (b) photos of supersonic flow in two-dimensional model of nozzle edge (Prandelt-Mayer expansion) $M_\infty = 1.56$

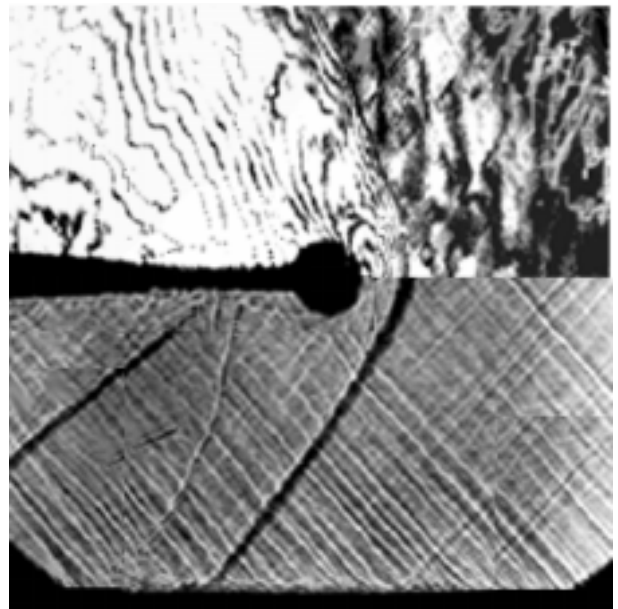
3.4 Calibration models

The test cone (Fig. 6a) has $\theta_c = 30^\circ$. The theoretical cone flow parameters behind shock wave are published in the ref [15] and it serves as referents values. Validation of the results obtained from holographic intereferogram recorded for $M_\infty = 1.56$ (fig 6a. in the space between point A and shock wave) is proof comparing with referents. The agreement is excellent (Table 3) [4,5].

Figure. 6b shows the isodensity lines around sphere in the flow with $M_{\text{exp}} = 1.06$. On the interferometric part of the photo easily noticeable are: the stagnation point, the detached bow wave, the vortex sheet generated behind the sphere and so on.



a)



b)

Figure 6. Composite interferometric-schlieren photos of flow around cone ($\theta_c = 30^\circ$) (a) and sphere $D = 26$ mm (b)

3.5 Flow around missile

In order to eliminate the appearance of a strong shock wave at a supersonic flight of a missile [12-14], which considerably increases the drag, a spike is mounted on its nose. The visualization of the flow was carried out for a supersonic flow with Mach number $M_\infty = 1.86$, Reynolds number $Re_d = 0.38 \cdot 10^6$, and for the angle of attack $\alpha = 0^\circ$ (fig. 7a).

Visualization experiments were performed in order to explain the obtained aerodynamic coefficients. From the interferogram it is clear that at the tip of the spike a conical shock wave is formed accompanied with a boundary layer separation downstream. Between the wave and the spike, a recirculation zone is formed. There is a strong deflection of the stream in the region of the boundary layer reattachment, provoking the

appearance of a curved separating shock wave, As a result of the interaction of this wave with the conical shock wave emanating from the tip, a new conical shock wave is formed. These elements of the flow can be seen from the schlieren photo, too.

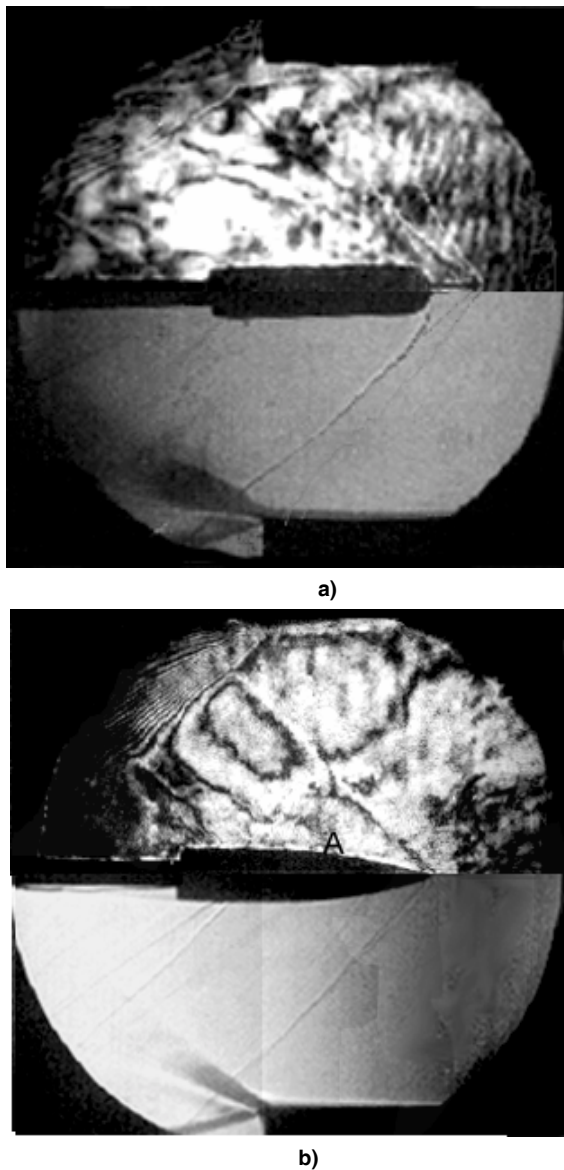


Figure 7. Composite iterferometric and schlieren photos of flow field around projectile with a spike mounted on its nose for $M_\infty = 1.86$ (a). The same for the hypothetical projectile 122 mm diameter and $M_\infty = 1.56$ (b)

The interferogram (fig 7b) of flow field of 122mm projectile is used for quantitative evaluation of flow pressure in the point A behind shock wave and above hole for pressure measurement ($x = 55.9$ mm, $y = 11.35$ mm), PMS gives the pressure $P_{st} = 25\ 028$ N/m², interferogram $P_{st} = 25\ 807$ N/m². The difference is about 3%.

3.6 Flow disturbed by slot

The test has been performed to determine how the flow is affected by presence of the single normal and slanted slot in the bottom plate of the test section of

wind tunnel T-36 [4,5,7,10]. The aim was only to visualize the disturbances in the external flow caused by slot. Two method have been used; schlieren and holographic interferometry. The free stream Mach number was $M_\infty = 0.83$. The disturbances in the flow are expressed in Figure 8a by variation of intensity and in Figure 8b, by distortion of parallel fringe system. A concentration of the fringes indicates the formation of the pressure wave. Interferogram precisely describes the disturbance, which reaches up to 60% of the test section height. That is not at all negligible, because the disturbance reaches even beyond the axis of test section. Figures 9a, b and c show the interferogram and the schlieren photos of the flow in presence of the cone-model in the test section with slot in the bottom wall.

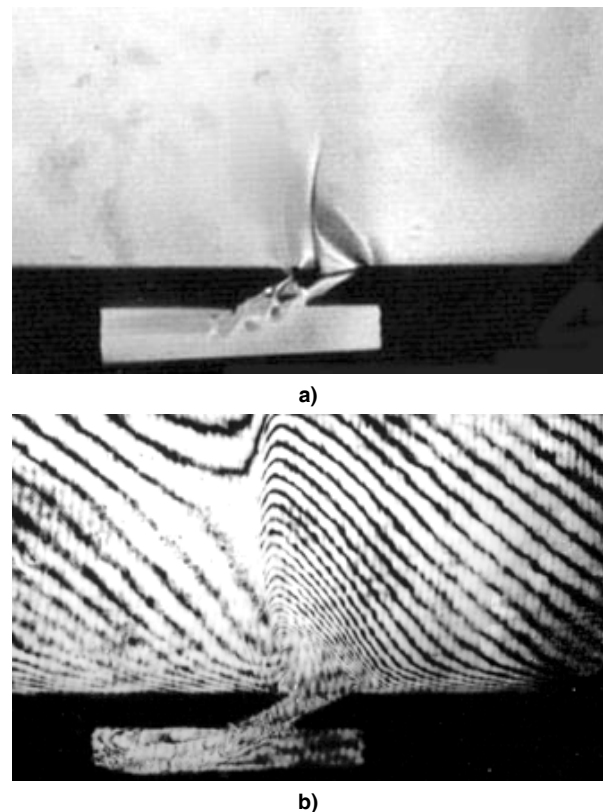


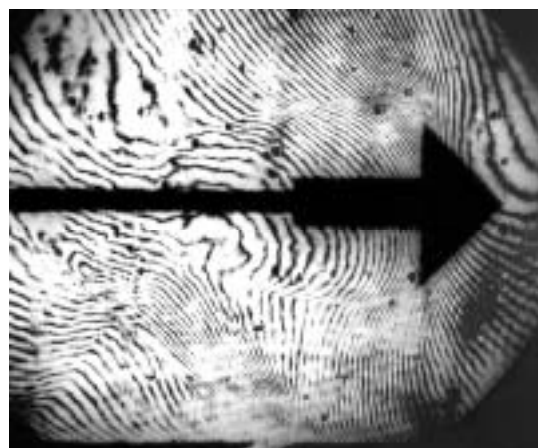
Figure 8. Schlieren and interferogram of flow caused by a slanted slot in the test section bottom; $M_\infty = 0.83$ Flow direction is from right to left.

4. CONCLUSION

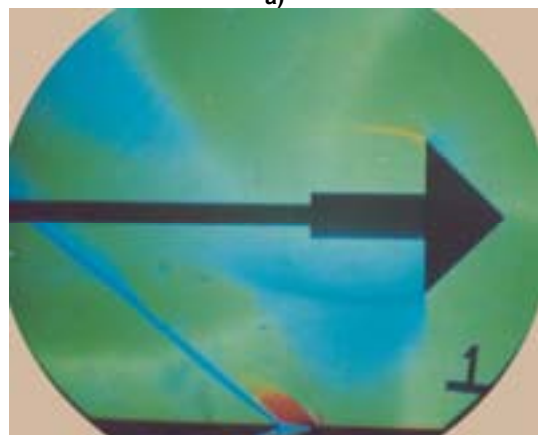
Testing of flow field around models in wind tunnels using the methods of holographic interferometry showed significant advantages of this method, compared with schlieren and other classical ones.

For two-dimensional and axially symmetrical fields one interferogram is enough to complete flow visualization and calculation. Schlieren method reduces three-dimensional flow to two-dimensional image and calculation become very complicated. Holographic interferometry gives best results for transonic and supersonic flows. For subsonic and hypersonic flows (with the weakly refraction and small air density) the results are worse. Holographic interferometry allows

agreat number of information with high accuracy from small number of experiments.



a)



b)



c)

Figure 9. Interferometric (a), schlieren (b), and composite (c) photos of flow field around cone $\theta_c = 90^\circ$, in the test section with sloped slot in the bottom wall for $M_\infty = 0.83$

REFERENCES

- [1] Marzkirich, W.: *Flow visualization*, Academic Press, New York, 1977:
- [2] Vest, C.M.: *Holographic Interferometry*, New York, Wiley and sons, 1982.
- [3] Settles, G.S: Modern Developments in Flow Visualization, *AIAA Journal*, vol. 24, No. 8, pp. 1313-1323, 1986.
- [4] Ristić, S.: Contribution to Development of Flow Visualization Methods Based on Laser Techniques,

doctoral thesis, ETF, University of Belgrade, 1993, (in Serbian).

- [5] Ristić, S.: Flow Visualization Technics in Wind Tunnels, Technical report, MTI, Belgrade, 1996.
- [6] Ristić, S.: Optical Flow Visualization Technics, Notes for a University Course, ETF, University of Belgrade, 1997.
- [7] Ristić, S.: Disturbance of Transonic wind Tunnel Flow by a Slot in the Tunnel Wall, *Experiments in fluids*, 11, pp. 403-405, 1990.
- [8] Ristić, S.: Testing of the Flow Field Around the Nozzle Edge Using the Method of Holographic Interferometry, *Fizika*, 22, 3, pp. 529-543, 1990.
- [9] Ristić, S., Srećković M.: Flow Investigation in 2D Model of Supersonic Nozzle by the Method of Holographic Interferometry, *Opto* 93, pp.101-110, Paris, 1993.
- [10] Ristić, S., Srećković M.: Pressure Disturbances Testing by Schlieren Method and Holographic Interferometry, *Laser '98*, 7-11, Tucson, Arizona, Proceedings pp. 568-547, 1998.
- [11] Ristić, S.: Quantitative Processing Optimization of Holographic interferograms od 2D and Axisymmetric Flow Field, *NTP*, Vol. 46, No. 4-5, pp. 73-86, 1996, (in Serbian).
- [12] Ristić, S.: Optical Methods In Flow Visualization, *Applied Physics in Serbia-APS*, Serbian Academy of Sciences and Arts, Scientific Meetings, vol. XCVIII, Department of mathematics, physics and geosciences, Book 2-1, pp. 143-146, 2002, (in Serbian).
- [13] Milićev, S., Pavlović, D., Ristić, S., Vitić, A.: On the Influence of Spike Shape at Supersonic Flow Past Blunt Bodies, *Facta Universitatis, series: Mechanics, Automatic, Control and Robotics*, Vol. 3, No. 12, pp. 371-382, 2002.
- [14] Milićev, S., Pavlović, D., Ristić, S., Vitić, A.: Experimental Study of the Influence of Spike Shape Axisymmetric Flow Past Bodies, *Theoretical and Applied Mechanics, Special Vol.1*, Proceedings of the 23rd Yugoslav Congress of Theoretical and Applied Mechanics, Belgrade, pp. 261-264, October, 2001.
- [15] Jones, D.J.: *Tables of Inviscid Supersonic Flow About Circular Cones at Incidence*, Agard 137, 1971.

ВИЗУАЛИЗАЦИЈА СТРУЈАЊА У АЕРОТУНЕЛИМА ОПТИЧКИМ МЕТОДАМА

Славица Ристић

У раду је разматрана примена оптичких метода: метод сенке, шлирен метод и холографска интерферометрија, у визуализацији струјања у аеротунелима. Приказано је неколико примера визуализације струјања у аеротунелима у ВТИ-у. Посебано су анализиране предности које има холографска интерферометрија у квантитативном испитивању струјног поља.

Table 2. Flow parameters in the supersonic nozzle [4]

Tap	x (mm)	Pressure measurements					Holographic interferometry			
		P (kg/m ²)	ρ_p (kg/m ³)	n_p	N_p	M_p	N_i	n_i	ρ_i (kg/m ³)	M_i
31	39.00	167.77	0.333	1.000075	34.88	1.83	33.00	1.000079	0.356	1.75
33	49.00	162.32	0.326	1.000073	35.51	1.85	35.00	1.000074	0.332	1.84
35	59.00	144.47	0.300	1.000067	37.62	1.92	37.00	1.000069	0.307	1.93
37	69.00	123.77	0.268	1.000060	40.16	2.02	39.00	1.000064	0.283	2.02
39	79.00	114.76	0.254	1.000057	41.30	2.07	41.00	1.000058	0.258	2.12
311	89.00	105.71	0.240	1.000054	42.47	2.12	42.00	1.000054	0.246	2.16
313	99.00	94.49	0.221	1.000050	43.97	2.19	43.50	1.000049	0.227	2.22
315	109.00	84.17	0.204	1.000046	45.39	2.27	45.00	1.000044	0.209	2.30
317	119.00	76.20	0.190	1.000043	46.52	2.33	46.00	1.000041	0.197	2.34
319	129.00	71.02	0.180	1.000041	47.28	2.37	47.00	1.000037	0.184	2.39
321	139.00	64.17	0.168	1.000038	48.30	2.44	48.00	1.000034	0.172	2.44
323	149.00	62.02	0.164	1.000037	48.62	2.46	49.00	1.000031	0.159	2.56

Table 3. Flow parameters around cone, $\theta_c = 15^\circ$ x = 30 mm, z = 9 - 29 mm, n = const [4]

Position		Holographic interferogram					AGARD 137 –theoretical [15]				
K	Y (mm)	N	n	P (kg/m ³)	V (m/s)	M	ρ (kg/m ³)	n	V (m/s)	M	N
11	29.	0.01	1.0001	0.051	415.025	1.450	0.0511	1.0001150	415.731	1.45	0.00
10	27.	0.05	1.0001	0.052	411.884	1.434	0.0523	1.0001177	411.040	1.43	0.05
9	25.	0.10	1.0001	0.053	408.747	1.419	0.0532	1.0001197	407.583	1.41	0.11
8	23.	0.15	1.0001	0.054	406.240	1.407	0.0539	1.0001214	404.553	1.40	0.17
7	21.	0.20	1.0001	0.054	403.736	1.395	0.0547	1.0001230	401.706	1.38	0.23
6	19.	0.25	1.0001	0.055	401.441	1.384	0.0554	1.0001246	398.877	1.37	0.29
5	17.	0.30	1.0001	0.055	398.732	1.371	0.0561	1.0001261	396.239	1.36	0.34
4	15.	0.35	1.0001	0.056	395.815	1.357	0.0567	1.0001277	393.562	1.35	0.39
3	13.	0.40	1.0001	0.057	392.275	1.340	0.0574	1.0001291	390.976	1.33	0.44
2	11.	0.45	1.0001	0.059	387.695	1.319	0.0580	1.0001304	388.717	1.32	0.48
1	9.	0.50	1.0001	0.060	380.825	1.288	0.0583	1.0001311	387.554	1.32	0.50